Chemical Engineering Journal 156 (2010) 380–387

Contents lists available at ScienceDirect

Chemical Engineering Journal

journal homepage: www.elsevier.com/locate/cej

Effect of different promoters on $Ni/CeZrO_2$ catalyst for autothermal reforming and partial oxidation of methane

Sandra C. Dantas, Janaína C. Escritori, Ricardo R. Soares, Carla E. Hori*

Faculdade de Engenharia Química, Universidade Federal de Uberlândia, Av. João Naves de Ávila, 2121, Bloco 1K, Campus Santa Mônica, CEP:38400-901, Uberlândia, MG, Brazil

ARTICLE INFO

Article history:
Received 15 July 2009
Received in revised form 19 October 2009
Accepted 21 October 2009

Keywords:
Promoters
Methane
Autothermal reforming
$Ni/CeZrO_2$

ABSTRACT

$Ni/CeZrO_2$ catalysts promoted by Ag, Fe, Pt and Pd were investigated for methane autothermal reforming and partial oxidation of methane. The catalysts properties were determined by BET surface area, X-ray diffraction (XRD), H_2 temperature-programmed reduction (TPR), temperature-programmed desorption of CO_2 (CO_2-TPD) and UV–vis diffuse reflectance spectroscopy (DRS). Nickel dispersions were evaluated using a model reaction, the dehydrogenation of cyclohexane. BET surface area results showed that the catalysts prepared by successive impregnation presented lower surface area which favored the smaller nickel dispersion. XRD analysis showed the formation of a ceria–zirconia solid solution. TPR experiments revealed that the addition of Pt and Pd as promoters increased the reducibility of nickel. CO_2-TPD results indicated that the AgNiCZ catalysts presented the best redox properties among all catalysts. The autothermal reforming of methane showed that, among different promoters, the sample modified with silver, AgNiCZ, presented higher methane conversion and better stability during the reaction. These results are related to the good reducibility and to the higher redox capacity observed in TPR and CO_2-TPD analysis. Samples prepared by successive impregnation technique resulted in a smaller catalytic activity. For partial oxidation of methane, just as happened in autothermal reforming, AgNiCZ also presented the best performance during the 24 h of reaction and the addition of silver by successive impregnation resulted in a lower methane conversion, probably, due to the smaller metal dispersion.

1. Introduction

In recent years, there has been much interest in hydrogen production for high efficiency generation of electricity in fuel cells [1]. Special attention has been given to fuel cells technology due to the fact that it does not have harmful emissions compared to other energy conversion systems [2]. Among all the potential sources of hydrogen, natural gas, composed largely by methane, offers many advantages: it is very abundant, clean and it can be easily converted to hydrogen [3].

Among several processes used to obtain hydrogen, steam methane reforming (SMR) shows the highest H_2-yield. However, it requires high energy input. On the other hand, catalytic partial oxidation (CPOX) releases energy, despite of a lower H_2/CO ratio. Since autothermal reforming (ATR) integrates both processes, it has attracted more attention in the last years. Seo et al. [4] analyzing the process of methane reforming to produce hydrogen through computer simulations, verified that partial oxidation and autothermal reforming of methane are more attractive than steam reforming, because they require less energy to produce the same amount of hydrogen.

Nickel supported on alumina catalysts are traditionally used for methane reforming reactions especially due to their low cost. However, these catalysts suffer severe deactivation generally because of the formation of carbon deposits on the surface. In order to improve the stability of these Ni/Al_2O_3 catalysts, CeO_2 and $CeZrO_2$ have been tried as supports since their oxygen storage properties help to avoid the accumulation of coke on the surface [5,6]. Recently, Chen et al. [7] studied the effect of preparation methods on structure and performance of $Ni/Ce_{0.75}Zr_{0.25}O_2$ catalysts for dry methane reforming, while Xu and Wang [8] analyzed the activity and coking resistance of $Ni/Ce_xZr_{1-x}O_2$ catalysts in partial oxidation of methane reaction. Both groups reported promising results for the use of nickel- and ceria-based catalysts for methane reforming reactions. Escritori et al. [9] investigated Ni/Al_2O_3, $Ni/CeO_2/Al_2O_3$, $Ni/CeZrO_2/Al_2O_3$ and $Ni/CeZrO_2$ samples for autothermal reforming of methane. They verified that $Ni/CeZrO_2/Al_2O_3$ catalysts were active at lower temperatures than Ni/Al_2O_3, since the mixed oxide offers more actives sites for the reaction.

Besides changing the support, another form to avoid coke deposition is the use of dopants such as noble metals [10,11]. It has been reported in the literature that the use of promoters such as Pt on Ni/Al_2O_3 for methane reforming with CO_2 and O_2 can increase

* Corresponding author. Fax: +55 34 3239 4188.
E-mail address: cehori@ufu.br (C.E. Hori).

1385-8947/$ – see front matter © 2009 Elsevier B.V. All rights reserved.
doi:10.1016/j.cej.2009.10.047

the activity and the stability of these catalysts [12]. Recently, Dias and Assaf [1] investigated the use of small amounts of palladium as a promoter for Ni/Al_2O_3 catalysts during the methane autothermal reforming. They verified that palladium is a good promoter since the catalytic activity was considerably increased. The use of silver as promoter was investigated by Parizotto et al. [13] and the results showed that this metal can contribute to the control of coke accumulation during methane reforming on nickel-based catalysts. The effect of the preparation methods on the properties of 0.3%Pt–10%Ni/Al_2O_3 catalysts was evaluated by Tomishige et al. [12]. They verified that a sample prepared by successive impregnation showed higher activity at lower temperatures than the bimetallic catalyst prepared by co-impregnation and the monometallic catalyst in the autothermal reforming of methane.

In order to try to combine the advantages of the use of a ceria-based support and the use of dopants to improve the performance of a nickel-based catalysts, we decided to study the effect of promoters such as platinum, palladium, silver and iron, on the properties and on the catalytic performance of $Ni/CeZrO_2$ for partial oxidation and autothermal reforming of methane.

2. Experimental

2.1. Catalyst preparation

The support, $CeZrO_2$, with atomic Ce/Zr ratio equals to 1, was prepared by co-precipitation technique, using $(NH_4)_2Ce(NO_3)_6$ and $ZrO(NO_3)_2$ as precursors and calcination at 773 K during 4 h. In order to evaluate the effect of the method of addition of the dopant we used two preparation methods: co-impregnation and successive impregnation. Co-impregnation was performed using an aqueous solution of nickel, silver, iron, platinum and palladium nitrates (10 wt.% for Ni and 0.1 wt.% for promoters). Then, the samples were dried at 393 K for 2 h and calcined in air at 723 K during 4 h. For the successive impregnation method, 10 wt.% nickel was added to the $CeZrO_2$ support and calcined. Then, successively, another impregnation was performed using a silver nitrate solution to obtain samples containing 0.1 and 1 wt.% of silver. The samples were dried and calcined as the catalysts prepared by co-impregnation method. The catalysts synthesized and the nomenclatures used in the present work are listed in Table 1.

2.2. Catalysts characterization

BET surface areas of the catalysts were measured using a Quantasorb Jr. apparatus equipped with a thermal conductivity detector. Before nitrogen adsorption, samples were pre-treated at 423 K, during 12 h. N_2 adsorption was carried through at liquid nitrogen temperature (77 K).

X-ray diffraction measurements were made using a RIGAKU diffractometer with a CuKα radiation. XRD data were collected at 0.04°/step with integration times of 1 s/step between $2\theta = 25°$ and 65°.

Table 1
Nomenclature used for the catalysts.

Catalyst	Used nomination
10%$Ni/CeZrO_2$	NiCZ
0.1%Ag–10%$Ni/CeZrO_2$	AgNiCZ
0.1%Fe–10%$Ni/CeZrO_2$	FeNiCZ
0.1%Pt–10%$Ni/CeZrO_2$	PtNiCZ
0.1%Pd–10%$Ni/CeZrO_2$	PdNiCZ
0.1%Ag–10%$Ni/CeZrO_2$ (successive impregnation)	AgNiCZ-s
1%Ag–10%$Ni/CeZrO_2$ (successive impregnation)	1AgNiCZ-s

Nickel dispersion was estimated through cyclohexane dehydrogenation, a structure insensitive reaction [14]. The samples (25 mg) were submitted to the same pretreatment (drying and reduction) as described in CO_2-TPD. After the reduction step, the sample was cooled in hydrogen flow to 523 K and the flow was increased to 100 mL/min. The reaction mixture was obtained by bubbling hydrogen through a saturator containing cyclohexane (99.9%) at 285 K (H_2/cyclohexane = 13.2). Reaction temperatures varied between 523 and 573 K. At these conditions, no mass transfer or equilibrium limitations were observed. The composition of effluent gas phase was measured by online gas chromatograph (Shimadzu) equipped with a thermal conductivity detector and a Chrompack CP-WAX 57 CB column.

Temperature-programmed reduction (TPR) measurements were carried out in a micro-reactor coupled to a quadrupole mass spectrometer (Balzers, Omnistar). A mixture of 2% H_2 in Ar flowed through the sample (300 mg) at 30 mL/min, raising the temperature at a heating rate of 10 K/min up to 1273 K. H_2 consumption was obtained from the integrated peak area of the reduction profiles relative to a calibration curve.

CO_2 temperature-programmed desorption (CO_2-TPD) measurements were carried out in a micro-reactor coupled to a quadrupole mass spectrometer (Balzers, Omnistar). The samples were reduced under H_2 flow (30 mL/min), increasing the temperature up to 773 K at 10 K/min. The temperature remained at 773 K for 3 h, the H_2 flow was replaced by He and the sample was heated up to 1073 K. Then, the samples were cooled to room temperature and the He flow was replaced by a mixture of 20%CO_2/He for chemisorption. After CO_2 chemisorption was completed, the reactor was purged with He and CO_2-TPD measurements were carried out increasing the temperature up to 1073 K at 20 K/min. CO_2 desorbed and CO produced were obtained from the integrated peak areas of the profiles relative to a calibration curve.

The samples were characterized at room temperature between 200 and 800 nm in a VARIAN-Cary 500 UV–vis spectrophotometer equipped with a diffuse reflectance accessory (Harrick). $CeZrO_2$ was used as reference, and the Kubelka–Munk function F(R) was calculated.

2.3. Autothermal reforming of methane

Before catalytic tests, the sample was reduced as described in the CO_2-TPD. After the reduction, the sample was heated to 1073 K under He (30 mL/min). The catalytic tests were carried out using 12 mg of catalyst and a total flow of 180 mL/min. The feed composition was $2CH_4{:}1H_2O{:}0.5O_2$. Effluent gases from the reactor were analyzed by a gas chromatograph (Shimadzu) equipped with a Hayesep column.

2.4. Partial oxidation of methane

Before catalytic tests, the sample was reduced as described in the CO_2-TPD. After the reduction, the sample was heated to 1073 K under He (30 mL/min). The catalytic tests were carried out using 6 mg of catalyst and a total flow of 300 mL/min. The feed composition was $2CH_4{:}1O_2$.

3. Results and discussion

Table 2 summarizes BET surface areas, NiO particle sizes and nickel metal dispersions obtained for all synthesized samples. The value of BET area of the $CeZrO_2$ support is similar to values previously reported in the literature [15]. The addition of metals to $CeZrO_2$ did not change significantly the total area. The samples prepared by successive impregnation method showed lower

Table 2
Results of BET area, NiO particle size and apparent metallic dispersion.

Catalyst	BET surface area (m^2/g_{cat})	Dp_{NiO} (nm)	Ni dispersion (%)
$CeZrO_2$	102	–	–
NiCZ	86	24	1.0
AgNiCZ	84	24	1.2
FeNiCZ	81	27	1.4
PdNiCZ	85	27	1.5
PtNiCZ	86	19	1.9
AgNiCZ-s	66	–	0.8
1AgNiCZ-s	75	–	0.2

values of BET areas. This small drop of BET areas is probably due to the blockage of some pores.

Fig. 1 presents XRD patterns obtained between $2\theta = 25^\circ$ and 65°. The samples showed similar diffraction patterns, with peaks characteristic of NiO at $2\theta = 37.2^\circ$, 43.2° and 63°. For the support, $CeZrO_2$, a shift in the position of the peaks relative to the cubic ceria phase to higher 2θ positions was observed. The peak with higher intensity shifted from $2\theta = 28.6^\circ$ to 29.3°, which indicates that zirconia was incorporated into CeO_2 lattice and formed a solid solution. Since the literature reports a peak position of 29.4° for ceria–zirconia solid solution with a Ce/Zr ratio equal to 1, it is possible that a highly dispersed zirconia phase is present and it was not detected [15]. X-ray diffraction patterns did not show significant effect of promoters, probably due to the small content used. NiO particle sizes were estimated using the Scherrer equation and the results are also presented in Table 2. All the samples presented large NiO particle sizes, probably due to the high Ni content used in this work.

Metal dispersions were estimated through the cyclohexane dehydrogenation model reaction (Table 2). These results are in agreement with BET surface area data. The samples prepared by successive impregnation, which presented smaller BET area, also had poorer nickel dispersion, probably due to the agglomeration of nickel particles on the surface of the carrier.

Fig. 2 presents H_2 consumption profiles during TPR experiments. Profile A was obtained for a bulk NiO sample, just to serve as a reference. In this sample, one can observe a peak with a maximum at 720 K and a shoulder around 830 K. These results are in agreement with the ones reported by Roh et al. [16]. They attributed this H_2 consumption to the reduction of nickel oxide to metal. For bulk $Ce_{0.5}Zr_{0.5}O_2$ (profile B), a large peak with maximum at 875 K was observed. This peak is generally attributed to the reduction of both surface oxide and bulk CeO_2, since it is known that the presence of Zr facilitates the reduction of ceria. These results are in agreement with the literature [9].

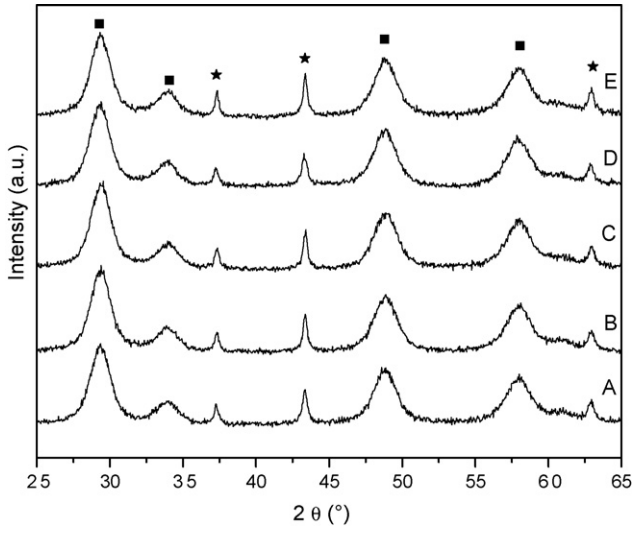

Fig. 1. X-ray diffraction profiles for NiCZ (A), FeNiCZ (B), AgNiCZ (C), PtNiCZ (D) and PdNiCZ (E), where (■) represents $CeZrO_2$ and (*) NiO.

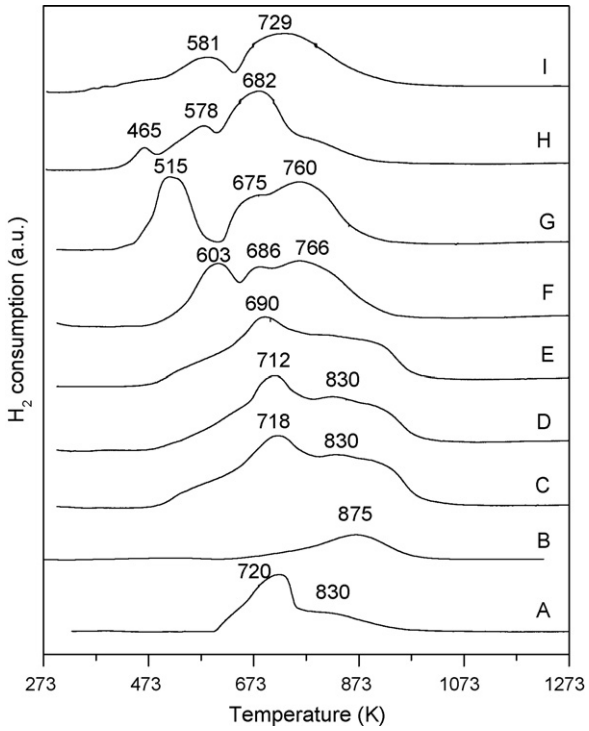

Fig. 2. H_2-TPR profiles: (A) NiO; (B) $CeZrO_2$; (C) NiCZ; (D) FeNiCZ; (E) AgNiCZ; (F) PtNiCZ; (G) PdNiCZ; (H) AgNiCZ-s and (I) 1AgNiCZ-s.

Despite of the small loadings of promoters used, their presence was enough to influence the reduction of the samples. NiCZ (profile C) showed a reduction peak around 720 K and a shoulder at 830 K. This TPR profile is in agreement with previous literature reports [17]. The reduction at lower temperature can be attributed to nickel oxide with low interaction with the support, while the reduction at higher temperature is assigned to the complex NiO species in intimate contact with $CeZrO_2$ [16]. The samples promoted by Ag and Fe (profiles D and E) showed similar behavior when compared with NiCZ.

PtNiCZ and PdNiCZ (profiles F and G) showed different reduction profiles when compared with others samples prepared by co-impregnation method. Pt and Pd promoters shifted the peak observed at 718 K for NiCZ to lower temperatures. For PtNiCZ, the reduction started around the same temperature than NiCZ, approximately 530 K. However, the first peak occurred at 603 K. For PdNiCZ, the reduction started at lower temperature than NiCZ, and the first peak occurred at 515 K. Passos et al. [18], studying catalysts of Pt supported on bulk $CeZrO_2$, reported a reduction peak at 503 K. This peak was attributed to the reduction of platinum oxide and to the reduction of $CeZrO_2$. The profile observed for PtNiCZ sample is not the simple addition of the NiCZ profile and $Pt/CeZrO_2$ observed in literature [18]. The same can be said for PdNiCZ sample. According to the literature [19], PdO reduces at room temperature and for a supported sample, $Pd/CeZrO_2$, the reduction appears around 410 K. The presence of noble metals, Pt and Pd, facilitated the reduction of the samples PdNiCZ and PtNiCZ. According to Dias and Assaf [1], which studied Ni/Al_2O_3 promoted with Pd, this result can be explained by the fact that Pd is easy to reduce. In the metallic state, Pd can easily adsorb hydrogen dissociatively. Thus, during the reduction process, metallic Pd is formed at lower temperatures than the necessary for the Ni^{2+} reduction. Therefore, the H formed on the

noble metal surface can move to nickel oxide surface, reducing it more easily.

The samples prepared by successive impregnation method showed different reduction profiles than the NiCZ and AgNiCZ samples. Profiles H and I presented more peaks at lower temperatures, indicating that the addition of silver made the samples easier to reduce. These results are in agreement with the literature on the reducibility of supported NiAg oxides [20]. According to Wojcieszak et al. [20], silver oxide is first reduced at low temperatures to form silver atoms on which H_2 molecules dissociate to highly reductive H atoms: these atoms are responsible for the reduction of nickel at lower temperatures.

Table 3 presents the values of hydrogen consumption during the TPR. The amount of H_2 necessary to complete NiO reduction is 1704 $\mu mol/g_{cat}$. The reducibilities of all samples, measured by H_2-TPR, were similar, with exception of the sample AgNiCZ-s. All catalysts presented H_2 consumptions above the theoretical value necessary to reduce just the nickel present. This result indicates that $CeZrO_2$ was also reduced during the analysis, which is in agreement with previous studies in the literature [21]. However, observing the consumption of the sample AgNiCZ-s, it may be noticed that this value is higher than the sum of the theoretical values to reduce both NiO and $CeZrO_2$. This result can be linked to the fact of that the successive addition of nickel and silver facilitated the reduction of the support, $CeZrO_2$, or hydrogen spillover may have occurred. According to Boaro et al. [22], the presence of metal might have modified strongly the characteristics of the support due the activation of the hydrogen on the metal and a posterior migration to the support. This phenomenon has been demonstrated in the presence of many supported metals, such as Ni, Ru, Rh, Pd, Pt, which adsorb hydrogen dissociatively [23].

The desorption profiles of CO_2 and CO are presented in Fig. 3. All profiles showed at least two peaks of CO_2 desorption, one at lower temperature (around 380 K) and another at higher temperature (around 600 K). CO_2 desorption is continuous between these two regions and after the maximum at higher temperature, the desorption continued until 800 K. This peak at lower temperature is probably due to the CO_2 desorption which was adsorbed on the support, and the second peak could be attributed to the CO_2 adsorbed on metallic nickel [24]. The profiles differ in relation to the intensity of the peak at the lowest temperature. For NiCZ, FeNiCZ and PdNiCZ, this peak is more accentuated. Unlike the others, the samples PtNiCZ and AgNiCZ do not present a great difference in the intensity of the desorption between the low and high temperature regions. AgNiCZ profile showed a practically constant CO_2 desorption signal between 380 and 650 K.

Table 3 presents quantitative results of CO_2-TPD and the maximum value of CO_2 dessorbed was 722 mole/g_{cat} for NiCZ catalyst, whereas the minimum value was 512 mole/g_{cat} detected for PtNiCZ sample. On the other hand, for the amount of CO desorbed, there was a larger variation and the catalyst that obtained higher CO desorption value was AgNiCZ. The production of CO during this analysis

Table 3
H_2 temperature-programmed reduction and CO_2 temperature-programmed desorption results.

Catalyst	H_2 consumption ($\mu mol/g_{cat}$)	CO_2-TPD ($\mu mol/g_{cat}$)	
		CO_2	CO
NiCZ	2226	722	330
AgNiCZ	2155	596	530
FeNiCZ	2144	670	85
PdNiCZ	2210	657	204
PtNiCZ	1837	512	252
AgNiCZ-s	3054	–	–
1AgNiCZ-s	1884	–	–

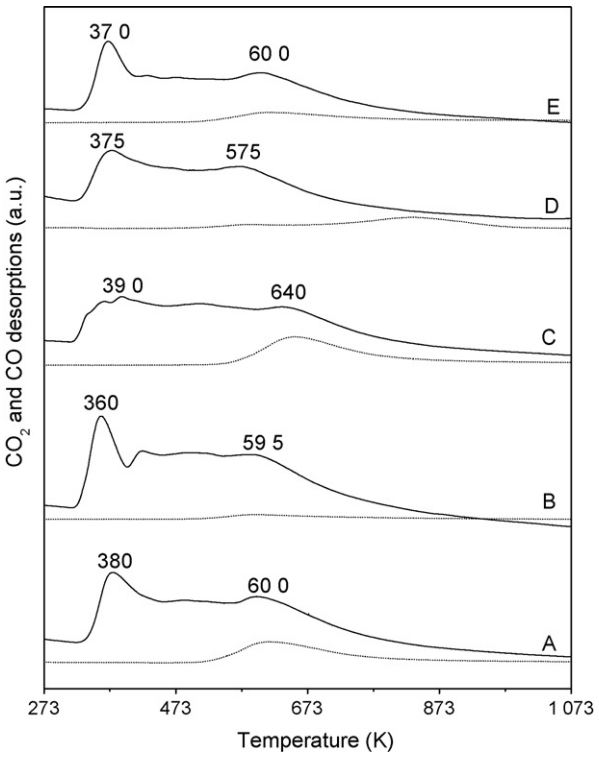

Fig. 3. Temperature-programmed desorption of CO_2 and CO profiles for the samples: (A) NiCZ; (B) FeNiCZ; (C) AgNiCZ; (D) PtNiCZ and (E) PdNiCZ (—) represents CO_2 signal and (. . .) CO signal.

can be explained by re-oxidation of the support. It is known that the amount of CO desorbed is directly related with the redox capacity of the sample. This occurs because the CO_2 adsorbed reacts with the vacancies of the support producing CO. In other words, the results of CO_2-TPD show a larger redox capacity for AgNiCZ catalyst. Hou and Yashima [25], analyzing catalysts of Ni/Mg/Al, observed that the increase of CO_2 adsorption may be correlated to the production of higher quantities of oxygen species on the catalyst surface, leading to higher activity and stability and low coke formation during the reforming of methane.

DRS analysis was used to identify the nickel species on the surface of the catalysts. The spectra of the catalysts are shown in Fig. 4, where the Kubelka–Munk functions of the corresponding bands are

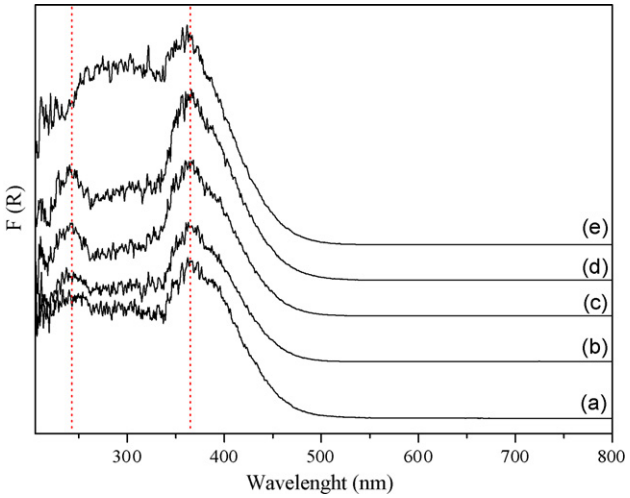

Fig. 4. UV–vis DRS profiles of catalysts: (A) NiCZ; (B) FeNiCZ; (C) PtNiCZ; (D) PdNiCZ and (E) AgNiCZ.

plotted as a function of the wavelength. All samples exhibited two bands around 225 and 475 nm. According to the literature, these absorption bands are usually ascribed to charge transfer of octahedral Ni^{2+} species in NiO lattices [26]. The occurrence of more intense bands at 360 nm may be attributed to the formation of NiO bulk, in others words, NiO with weak interaction with the support [27]. These results are in agreement with the low values of metal dispersion measured by cyclohexane dehydrogenation. All samples showed NiO bulk formation, which lead to a lower nickel dispersion on the surface of the carrier.

Fig. 5 presents methane conversions as a function of time during autothermal reforming catalytic tests. It may be noticed that there was not a great difference in the conversion of the methane among the catalysts, and that all the catalysts presented similar initial activities. AgNiCZ presented higher conversion of methane than the others, around 55%. PtNiCZ presented great stability in methane conversion, in the order of 47%. The highest activity observed for AgNiCZ could be attributed to the best redox capacity presented during CO_2-TPD. On the other hand, FeNiCZ presented strong deactivation during the reaction, and at the end of 24 h, the conversion was only 35%.

CO and CO_2 selectivities are shown in Fig. 6. All catalysts have a high selectivity for CO and a low selectivity for CO_2. Notice that CO and CO_2 selectivities add up to 100%, indicating low carbon deposition. NiCZ presented the smallest CO selectivity, around 82%. All the samples presented stable CO and CO_2 selectivities throughout the 24 h reaction period. H_2 selectivities were similar for all the catalysts, around 78%.

The similarity for methane conversion results for samples promoted by different metals could be related to similar nickel dispersions, to the use of the same $CeZrO_2$ support, and to the very small amount of promoters used. All this lead to samples with very similar numbers of Ni and $CeZrO_2$ sites, that are responsible for the dissociation of methane and others reagents. However, the stability of the catalysts can be explained by the redox capacities as presented in CO_2-TPD. AgNiCZ presented larger redox capacity and it was the most active during the catalytic tests. In the other extreme, the sample promoted with iron, that presented the smallest redox capacity, was the only one that suffered deactivation during 24 h of reaction. Nevertheless, the addition of promoters may have caused structural changes contributing to alter the activity and stability

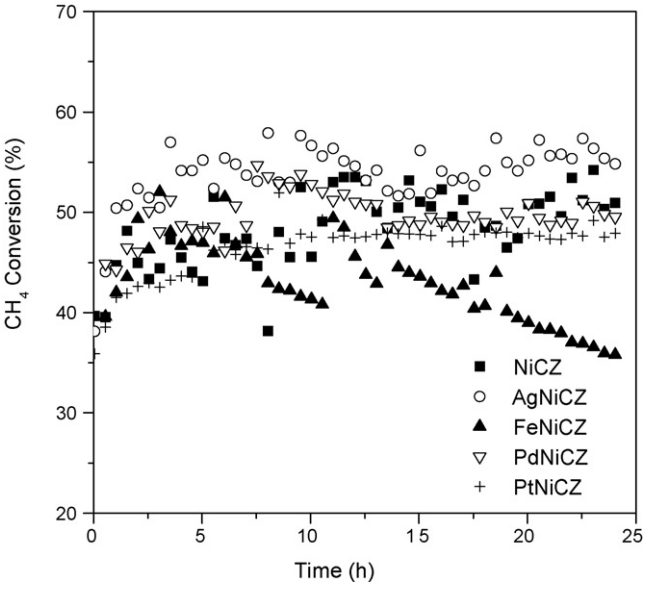

Fig. 5. CH_4 conversion during autothermal methane reforming at 1073 K.

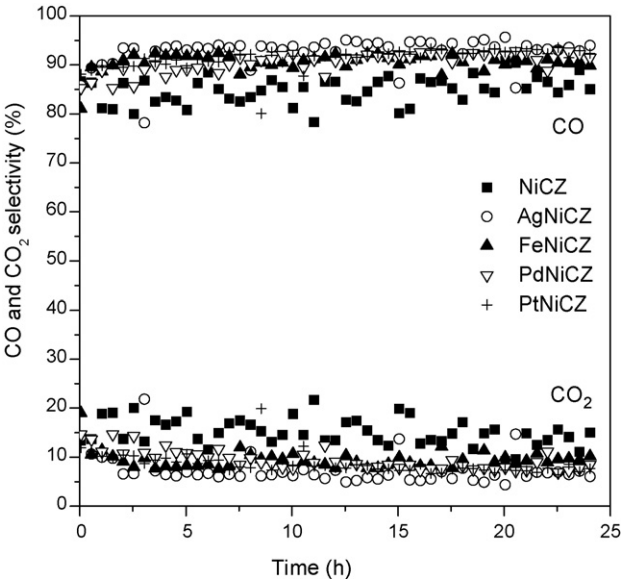

Fig. 6. CO and CO_2 selectivities during autothermal methane reforming at 1073 K.

of the catalysts. This is in agreement with the study presented by Larsen and Chorkendorff [28]. They observed that the presence of Ag, Pt or Pd with Ni favors the formation of a metal alloy on the surface. On the other hand, Fe and Ni mixture favors the formation of a metal alloy in which the adsorbed atoms (in this case, Fe atoms) migrate to the bulk phase for thermodynamical reasons. However, they also point out that the surrounding gas may have an important effect on the composition of the surface and it can create a chemical potential for adsorbate atoms staying at the surface. Nerlov and Chorkendorff [29] analyzed the case of Ni deposited on Cu for methanol synthesis using various mixtures containing CO_2, CO, and H_2. They verified that the presence of CO in the reaction feed leads to segregation of Ni to the surface, whereas this is not the case when only CO_2 and H_2 are fed. The authors concluded that CO acts strictly as a promoter in the system and the increase in activity can be correlated to the segregation of Ni to the surface. Since in our reaction conditions, we produce CO, these results may be an indication that, in the case of Fe and Ni mixture, Fe atoms stayed at the surface during autothermal reforming reaction. Since Fe is not very active for autothermal reforming of methane, the presence of Fe on the surface could have contributed to the deactivation observed during the reaction.

For the samples promoted by silver obtained through a different technique (Fig. 7), noticed that the addition of 0.1 wt.% Ag by successive impregnation resulted in a smaller catalytic activity. However, for Ag loadings of 1%, the sample presented a behavior similar to NiCZ catalyst. Parizotto et al. [13] studied Ni/Al_2O_3 catalysts promoted by Ag for steam reforming of methane. They verified that the addition of silver reduced the catalytic activity, and as the Ag content was increased there was a stronger decrease in catalytic activity. The authors also observed that the catalysts containing Ag presented an exceptional resistance to carbon deposition. According to the authors [13], the high stability of Ni catalysts promoted with Ag can be attributed to the combination of different effects: (i) the decrease of Ni ensemble; (ii) the change of superficial structure of Ni sites to the growth of graphitic structures and (iii) the equilibration of the different steps of reaction rate with the decrease of the C^* formation rate.

Fig. 8 presents CO and CO_2 selectivities obtained during autothermal reforming of methane. All catalysts showed high selectivity for CO and a low selectivity for CO_2 and these values were stable during 24 h of reaction. H_2 selectivities (not shown) were

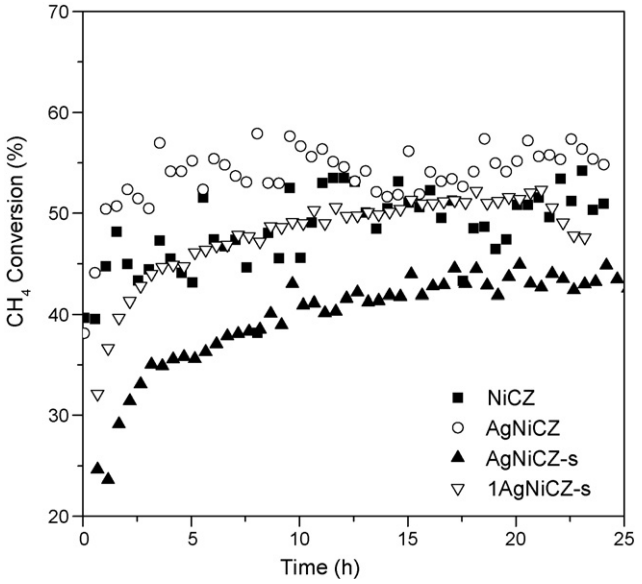

Fig. 7. CH_4 conversion during autothermal methane reforming at 1073 K for the catalysts promoted by silver.

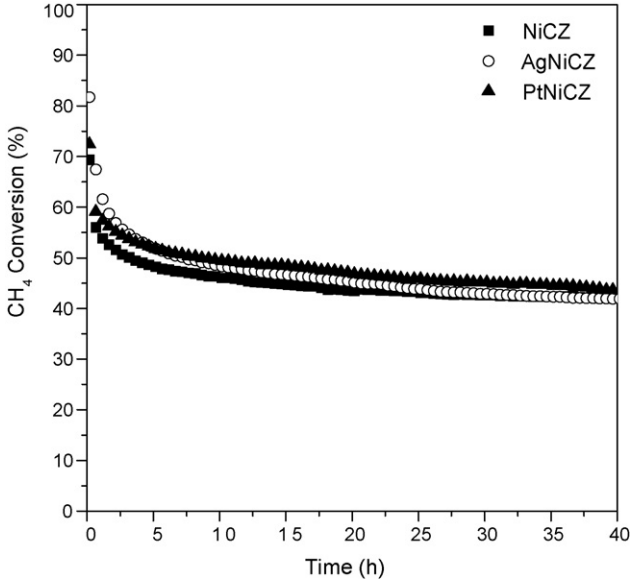

Fig. 9. CH_4 conversion during partial oxidation of methane at 1073 K.

high (around 80% for the samples NiCZ, AgNiCZ and AgNiCZ-s and 70% for 1AgNiCZ-s) and also quite stable. Summarizing, the catalyst promoted by silver through co-impregnation technique showed higher conversion and good H_2 and CO selectivities. This result can be related to the good reducibility and to the high redox capacity of this catalyst.

Fig. 9 presents methane conversions as a function of time during partial oxidation of methane for catalysts promoted with Ag and Pt. In general, the effect of 0.1% of different promoters was not enough to influence the results of partial oxidation of methane, because the used conditions were severe for these catalysts. The sample promoted with silver was, initially, the most active. However, after 40 h of reaction all catalysts had similar methane conversions, around 45%.

The similarity for methane conversion results, presented in Fig. 9, could be related to similar metallic dispersions and BET areas. According to Mattos et al. [30], the partial oxidation of methane reaction is directly related to metallic dispersion, that is, for higher metal dispersions, the conditions for methane dissociation and the formation of H_2 and CO are better. Xu and Wang [8], studying catalysts of Ni supported on CeO_2, ZrO_2 and $Ce_xZr_{1-x}O_2$, verified that for high temperatures the catalytic activity was dependent on BET area and Ni dispersion on the catalyst surface. Due to the small differences in dispersions and BET areas, the catalysts showed similar performances during partial oxidation of methane reaction.

Fig. 10 presents CO and CO_2 selectivities obtained during partial oxidation of methane. AgNiCZ presented, initially, smaller CO selectivity than the others, while PtNiCZ presented a little higher CO selectivity, around 90%. However, in general, all catalysts showed high selectivity for CO and a low selectivity for CO_2 and these values were stable during 40 h of reaction. The values of H_2 selectivities (not shown) were 40, 43 and 45% for the samples Ni/CZ, AgNiCZ and PtNiCZ, respectively. The results of H_2, CO and CO_2 selectivities can be explained by mechanism of the partial oxidation of methane

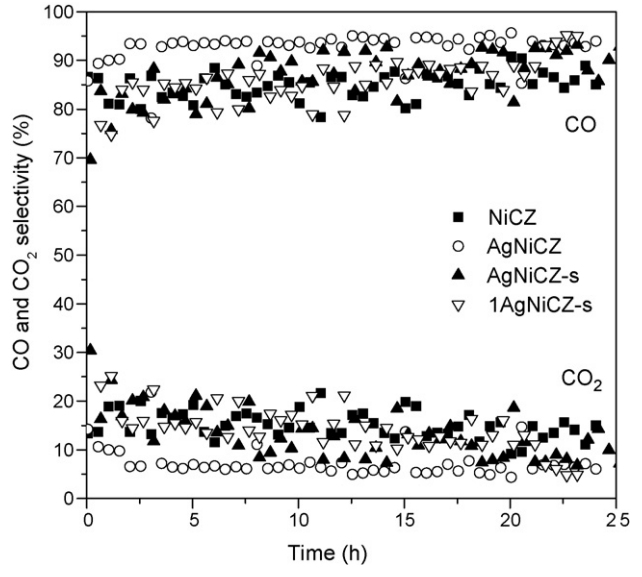

Fig. 8. CO and CO_2 selectivities during autothermal methane reforming at 1073 K for the catalysts promoted by silver.

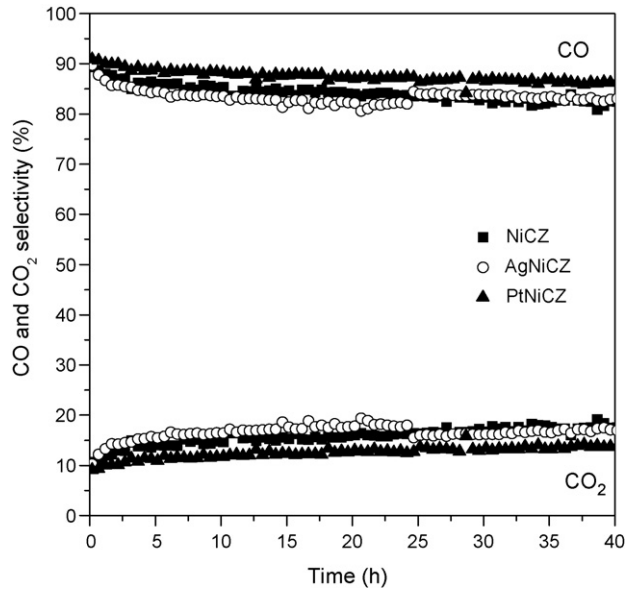

Fig. 10. CO and CO_2 selectivities during partial oxidation of methane at 1073 K.

reaction suggested by Mattos et al. [30] that happens concomitantly with the water gas shift inverse reaction.

Fig. 11 presents methane conversions as a function of time during partial oxidation of methane for samples promoted with silver. AgNiCZ was, initially, the most active. However, after 24 h reaction period, NiCZ and AgNiCZ had similar methane conversions, around 50%. The addition of silver by successive impregnation resulted in lower methane conversion during all the 24 h of reaction. These results are in agreement with the literature, since the activity for partial oxidation of methane is usually correlated to metal dispersion values [30].

Fig. 12 showed CO and CO_2 selectivities for catalysts promoted by silver. 1AgNiCZ-s presented CO selectivity slightly decreasing during 24 h of reaction and inverse behavior for CO_2 selectivity. As happened in POM for different metals promoters, all samples promoted by silver presented low selectivity to CO_2 formation and high selectivity to CO, presenting stable during the reaction.

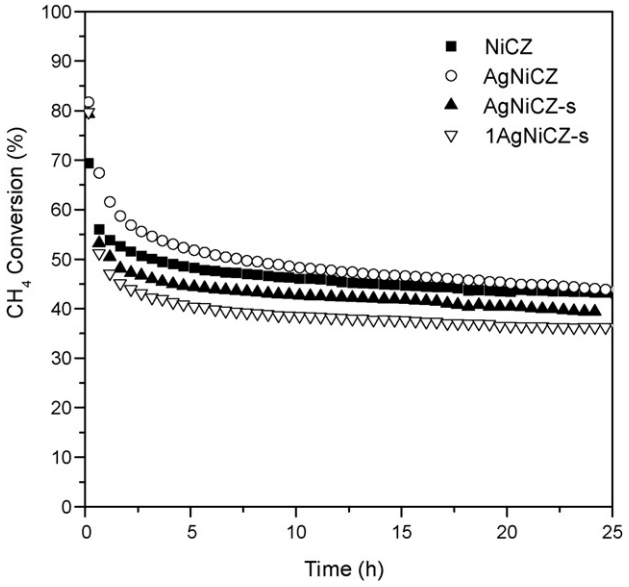

Fig. 11. CH_4 conversion during partial oxidation of methane at 1073 K for the catalysts promoted by silver.

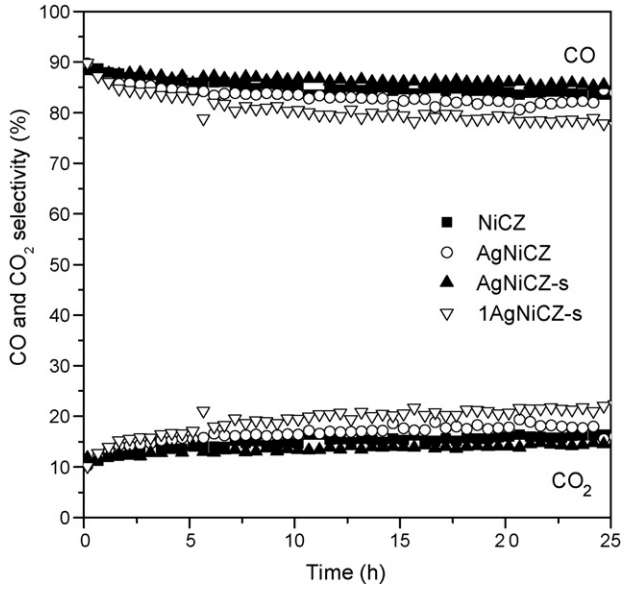

Fig. 12. CO and CO_2 selectivities during partial oxidation of methane at 1073 K for the catalysts promoted by silver.

The results of partial oxidation of methane showed that the promoted catalysts presented similar performance during this reaction. These results are related to the similar values of dispersions and BET areas. The samples promoted by silver, for successive impregnation technique, presented smaller methane conversion than the others, which is in agreement with the results of BET area and metallic dispersion.

4. Conclusions

In general, the addition of promoters to NiCZ catalyst did not influenced the BET area, NiO particle size and metallic dispersion, probably due to the small load of promoters used in this present study. XRD patterns revealed the formation of a ceria–zirconia solid solution. TPR results showed that the support was also reduced in this analysis and some promoters, as Pt and Pd, promote nickel and support reduction. AgNiCZ showed the best redox capacity, due to higher CO and CO_2 desorption in CO_2-TPD. Autothermal methane reforming revealed that among all catalysts, AgNiCZ presented higher values of methane conversion and stability during the reaction. These results are related to the good reducibility and to the higher redox capacity observed in TPR and CO_2-TPD analysis. For partial oxidation of methane, just as observed in autothermal reforming, AgNiCZ also presented the best performance during the 24 h of reaction and the addition of silver by successive impregnation resulted in a lower methane conversion, probably, due to the smaller values of metal dispersion.

Acknowledgments

The authors wish to acknowledge the financial support of Fapemig - Brazil (Fundação de Amparo à Pesquisa do Estado de Minas Gerais) through project TEC 785/2004. S.C. Dantas acknowledges her scholarship also provided by Fapemig–Brazil.

References

[1] J.A.C. Dias, J.M. Assaf, Autothermal reforming of methane over Ni/γ-Al_2O_3 promoted with Pd. The effect of the Pd source in activity, temperature profile of reactor and in ignition, Applied Catalysis A: General 334 (2008) 243–250.
[2] D.L. Hoang, S.H. Chan, O.L. Ding, Hydrogen production for fuel cells by autothermal reforming of methane over sulfide nickel catalyst on a gamma alumina support, Journal of Power Sources 159 (2006) 1248–1257.
[3] A.L. Dicks, Hydrogen generation from natural gas for the fuel cell systems of tomorrow, Journal of Power Sources 61 (1996) 113–124.
[4] Y.-S. Seo, A. Shirley, S.T. Kolaczkowski, Evaluation of thermodynamically favourable operating conditions for production of hydrogen in three different reforming technologies, Journal of Power Sources 108 (2002) 213–225.
[5] N. Laosiripojana, S. Assabumrungrat, Methane steam reforming over Ni/Ce-ZrO_2 catalyst: Influences of Ce-ZrO_2 support on reactivity, resistance toward carbon formation, and intrinsic reaction kinetics, Applied Catalysis A: General 290 (2005) 200–211.
[6] J. Gao, J. Guo, D. Liang, Z. Hou, J. Fei, X. Zheng, Production of syngas via autothermal reforming of methane in a fluidized-bed reactor over the combined CeO_2–ZrO_2/SiO_2 supported Ni catalysts, International Journal of Hydrogen Energy 33 (2008) 5493–5500.
[7] J. Chen, Q. Wu, J. Zhang, J. Zhang, Effect of preparation methods on structure and performance of Ni/$Ce_{0.75}Zr_{0.25}O_2$ catalysts for CH_4-CO_2 reforming, Fuel 87 (2008) 2901–2907.
[8] S. Xu, X. Wang, Highly active and coking resistant Ni/CeO_2-ZrO_2 catalyst for partial oxidation of methane, Fuel 84 (2005) 563–567.
[9] J.C. Escritori, S.C. Dantas, R.R. Soares, C.E. Hori, Methane autothermal reforming on nickel–ceria–zirconia based catalysts, Catalysis Communications 10 (2009) 1090–1094.
[10] D.L. Trimm, Catalysts for the control of coking during steam reforming, Catalysis Today 49 (1999) 3–10.
[11] R. Jens, Rostrup-Nielsen, Ib Alstrup, Innovation and science in the process industry Steam reforming and hydrogenolysis, Catalysis Today 53 (1999) 311–316.
[12] K. Tomishige, S. Kanazawa, M. Sato, K. Ikushima, K. Kunimori, Catalyst design of Pt-modified Ni/Al_2O_3 catalyst with flat temperature profile in methane reforming with CO_2 and O_2, Catalysis Letters 84 (2002) 69–74.

[13] N.V. Parizotto, K.O. Rocha, S. Damyanova, F.B. Passos, D. Zanchet, C.M.P. Marques, J.M.C. Bueno, Alumina-supported Ni catalysts modified with silver for the steam reforming of methane: effect of Ag on the control of coke formation, Applied Catalysis A: General 330 (2007) 12–22.
[14] F.A. Silva, D.S. Martinez, J.A.C. Ruiz, L.V. Mattos, C.E. Hori, F.B. Noronha, The effect of the use of cerium-doped alumina on the performance of $Pt/CeO_2/Al_2O_3$ and $Pt/CeZrO_2/Al_2O_3$ catalysts on the partial oxidation of methane, Applied Catalysis A: General 335 (2008) 145–152.
[15] C.E. Hori, H. Permana, K.Y. Simonng, A. Brenner, K. More, K.M. Rahmoeller, D. Belton, Thermal stability of oxygen storage properties in a mixed CeO_2-ZrO_2 system, Applied Catalysis B: Environmental 16 (1998) 105–117.
[16] H.S. Roh, K.W. Jun, W.S. Dong, J.S. Chang, S.E. Park, Y.I. Joe, Highly active and stable Ni/Ce-ZrO_2 catalyst for H_2 production from methane, Journal of Molecular Catalysis A: Chemical 181 (2002) 137–142.
[17] W.S. Dong, H.S. Roh, K.W. Jun, S.E. Park, Y.S. Oh, Methane reforming over Ni/Ce-ZrO_2 catalysts: effect of nickel content, Applied Catalysis A: General 226 (2002) 63–72.
[18] F.B. Passos, E.R. Oliveira, L.V. Mattos, F.B. Noronha, Partial oxidation of methane to synthesis gas on $Pt/Ce_xZr_{1-x}O_2$ catalysts: the effect of the support reducibility and of the metal dispersion on the stability of the catalysts, Catalysis Today 101 (2005) 23–30.
[19] L.S.F. Feio, J.C. Escritori, F.B. Noronha, C.E. Hori, Combustion of butyl carbitol using supported palladium catalysts, Catalysis Letters 120 (2008) 229–235.
[20] R. Wojcieszak, S. Monteverdi, J. Ghanbaja, M.M. Bettahar, Study of Ni–Ag/SiO_2 catalysts prepared by reduction in aqueous hydrazine, Journal of Colloid and Interface Science 317 (2008) 166–174.
[21] E. Aneggi, M. Boaro, C. de Leitenburg, G. Dolcetti, A. Trovarelli, Insights into the redox properties of ceria-based oxides and their implications in catalysis, Journal of Alloys and Compounds 408–412 (2006) 1096–1102.
[22] M. Boaro, M. Vicario, C. Leitenburg, G. Dolcetti, A. Trovarelli, The use of temperature-programmed and dynamic/transient methods in catalysis: characterization of ceria-based, model three-way catalysts, Catalysis Today 77 (2003) 407–417.
[23] U. Roland, T. Braunschweig, F. Roessner, On the nature of spilt-over hydrogen, Journal of Molecular Catalysis A: Chemical 127 (1997) 61–84.
[24] S.G. Wang, D.B. Cao, W.Y. Li, J. Wang, H. Jiao, CO_2 Reforming of CH_4 on Ni(111): A Density Functional Theory Calculation, Journal of Physical Chemistry B 110 (2006) 9979–9983.
[25] Z. Hou, T. Yashima, Meso-porous Ni/Mg/Al catalysts for methane reforming with CO_2, Applied Catalysis A: General 261 (2004) 205–209.
[26] L.P.R. Profeti, J.A.C. Dias, J.M. Assaf, E.M. Assaf, Hydrogen production by steam reforming of ethanol over Ni-based catalysts promoted with noble metals, Journal of Power Sources 190 (2009) 525–533.
[27] J.S. Lisboa, D.C.R.M. Santos, F.B. Passos, F.B. Noronha, Influence of the addition of promoters to steam reforming catalysts, Catalysis Today 101 (2005) 15–21.
[28] J.H. Larsen, I. Chorkendorff, From fundamental studies of reactivity on single crystals to the design of catalysts, Surface Science Reports 35 (1999) 163–222.
[29] J. Nerlov, I. Chorkendorff, Methanol synthesis from CO_2, CO, and H_2 over Cu(1 0 0) and Ni/Cu(1 0 0), Journal of Catalysis 181 (1999) 271–279.
[30] L.V. Mattos, E.R. Oliveira, P.D. Resende, F.B. Noronha, F.B. Passos, Partial oxidation of methane on Pt/Ce-ZrO_2 catalysts, Catalysis Today 77 (2002) 245–256.